Development and Field Test of Teleoperated Mobile Robots for Active Volcano Observation

Keiji Nagatani[1], Ken Akiyama[1], Genki Yamauchi[1], Kazuya Yoshida[1], Yasushi Hada[2], Shin'ichi Yuta[3], Tomoyuki Izu[4], and Randy Mackay[5]

***Abstract*— When an active volcano erupts, a restricted area is typically set according to the eruption level. However, it is very important to observe eruption products inside of this area to predict the timing and scale of volcanic hazards, such as debris flows. Therefore, we propose a robotic observation system for active volcanoes that is composed of a multi-rotor unmanned aerial vehicle (UAV) and a mobile ground robot. To deliver the ground robot safely from the multi-rotor UAV to the ground, we implemented a sky-crane mechanism and confirmed the feasibility of the mechanism theoretically. In this paper, we introduce our volcano observation scenario as well as the observation system and sky-crane mechanism we have developed. Finally, we report on a field test conducted at Mount Asama in September 2013.**

I. INTRODUCTION

In Japan, there are 110 active volcanoes, one fifteenth of all active volcanoes in the world. In 2009, the Japan Meteorological Agency identified 47 volcanic mountains [1] at which it is necessary to have a surveillance system in place. If one of the active volcanoes erupts in Japan, a restricted area is set. The size of the area is proportional to the scale of the eruption for observers' safety. On the other hand, it is very important to observe eruptive conditions and products inside of the restricted area, such as debri flows, to predict the timing and scale of volcanic disasters so that residents can be warned to evacuate. Recently, many fixed observation devices have been installed on the selected active volcanoes for remote observation. However, in emergency cases, there are no guarantees that these devices will work during eruption. Furthermore, it is sometimes difficult to estimate where craters will build up. Therefore, movable remote observation devices (teleoperated robots) in volcanic areas are required.

There have been some previous research studies on volcano exploration using mobile robotic technology. The best-known is the "Dante project," organized by Carnegie Mellon University. They used a walking mechanism with multiple legs[2]. This mechanism provided good traversal performance on rough terrain, and several field experiments were conducted to prove its reliability. After the eruption of Mount Unzen in Japan in 1990, unmanned construction machines were used to build mudslide-control dams to prevent damage from debris flow[3]. The machines have been improved continuously, and the technology was used in the nuclear disaster field in Fukushima in 2011. These machines are difficult to deploy rapidly for observation of volcanic disasters. In Europe, there was a large project called Robovolc that was designed to help scientists explore volcanoes[4][5]. It explored Mount Etna in September 2002. In that project, a small ground robot was used, but its ability to traverse rough terrains seemed limited.

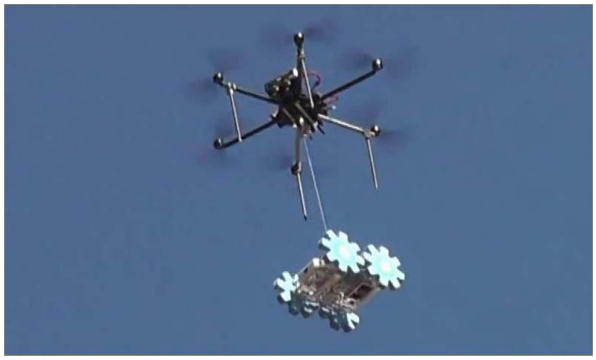

Fig. 1. Small mobile robot carried by a hexa-rotor UAV

An unmanned aerial vehicle (UAV) has the potential for use in volcanic observation, and Yamaha's UAV, called Rmax, was used practically for the observation of eruption at Mount Usu, in 2000[6]. Currently, the Rmax is the most significant aircraft for remote-observation at disaster sites in Japan. However, the UAV uses a gasoline engine, which cannot work at elevations above 1,000 m because of the decreased oxygen density at high altitudes. Some active volcanoes in Japan are located at high altitudes, so this system cannot be directly applied to them. On the other hand, recent research on electrically powered multi-rotor UAVs has become widespread globally, and battery performance is rapidly being improved. This type of UAV does not have a problem with low oxygen density.

Based on the requirements of the situation described above, our research group has been researching and developing small mobile ground robots for observation in the

* This work is supported by the Erosion Control Engineering division of the R&D Institution of River Technology in the Kanto Regional Development Bureau, Ministry of Land, Infrastructure, Transport, and Tourism. The field experiment at Mt.Asama was supported by the Earthquake Research Institute of the University of Tokyo.

[1] The graduate school of Engineering, Tohoku University, 6-6-01, Aramaki-Aoba, Aoba-ku, Sendai, Miyagi 980-8579, Japan (keiji@ieee.org)

*[2] Kogakuin University, 1-24-2, Nishi-shinjuku, Shinjuku, Tokyo, Japan (had@cc.kogakuin.ac.jp)

*[3] Shibaura Institute of Technology, 3-7-5, Toyosu, Koto-ku, Tokyo, Japan (yuta.shinichi@gmail.com)

*[4] enRoute Co., Ltd., 1-3-29 Ureshino, Fujimino, Saitama, Japan (izu@enroute.co.jp)

*[5] Japan Drones Co., Ltd., 1019-396, Karuizawa, Karuizawa-cho, Kita-Saku-gun, Nagano, Japan (rmackay9@japandrones.com)

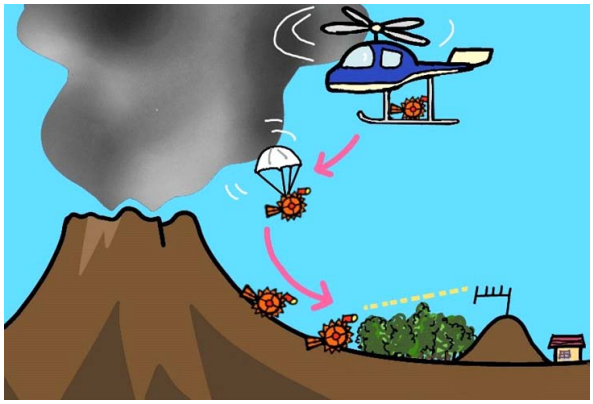

Fig. 2. A scenario for volcano exploration using a UAV and ground robot

Fig. 3. Hexa-rotor UAV "ZionPro800"

restricted areas of active volcanoes and has conducted some field tests, reported in [7] and [8]. In the previous field test in September 2013, we succeeded in a demonstration in which an electrically powered UAV delivered a small ground robot to the surface of Mount Asama (Fig.1). The ground robot explored the environment and obtained visual information based on teleoperation. In this paper, we introduce a robotic observation system for volcanic areas that we have developed and report on the field test.

II. Observation Scenario for Active Volcanoes

According to the Volcano and Debris Flow Research Team in the Public Works Research Institute (PWRI) of Japan, movable remote observation devices are expected to carry out the following tasks:

1) Sampling eruption products (i.e., determining what kind of eruption products are piled up) at several locations
2) Observing the situation of eruption products (quantity of eruption products, or snow in winter season, piled up)
3) Measuring the penetration capability of water (the extent to which the eruption products allow the passage of water)
4) Observing development of rill and gully erosion

These measurements allow estimation of the timing and scale of debris flows caused by the eruption products of volcanoes (or snow melting debris flow). However, with present technologies, it is difficult to perform all of the measurements described above. Therefore, in our research group, we aim to achieve measurements 2) and 4) by obtaining visual images using teleoperated mobile robots. One possibility is to use a high-resolution camera mounted on a UAV only; however, it is very important to have closed and stereoscopic images from the ground, according to a researcher in PWRI. Therefore, we propose a robotic surveillance scenario in restricted areas using a teleoperated small ground robot delivered by a UAV. An initial conceptual illustration of the scenario is shown in Fig.2.

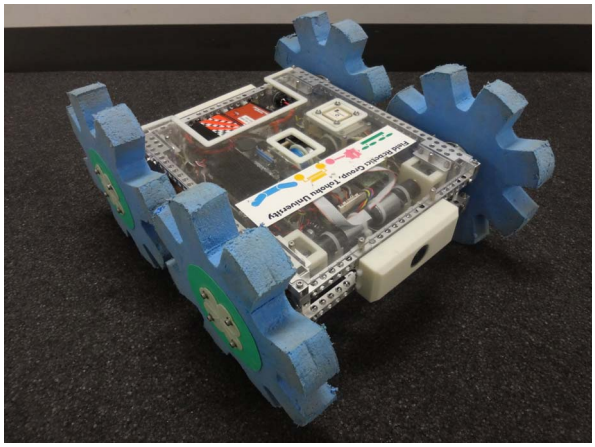

Fig. 4. Overview of volcano exploration robot CLOVER

III. Development of the Robotic Observation System

A. UAV to transport and deploy a ground robot

In many cases, an observation target area is at an elevation of over 1,000 m. In such environments, a gasoline engine UAV, such as the Rmax (Yamaha), cannot be used because of the reduction in combustion efficiency caused by low oxygen density. Therefore, in this study, we use an electrically powered multi-rotor UAV. Our target UAV is a ZionPro800 produced by EnRoute Co. Ltd., shown in Fig.3. It is a six-propeller-driven aircraft, with a payload capacity of 4-5 kg. The UAV is mounted with an Arduino microcontroller with the Arducopter software, which allows it to navigate autonomously based on GPS signals.

TABLE I
Specifications of CLOVER

L × W × H	450 mm × 360 mm × 220 mm
Weight	2.5-3.0 kg
Wheel	ϕ220 mm × W30 mm
Power source	$LiFePO_4$ (13.2V, 2300 mAh)

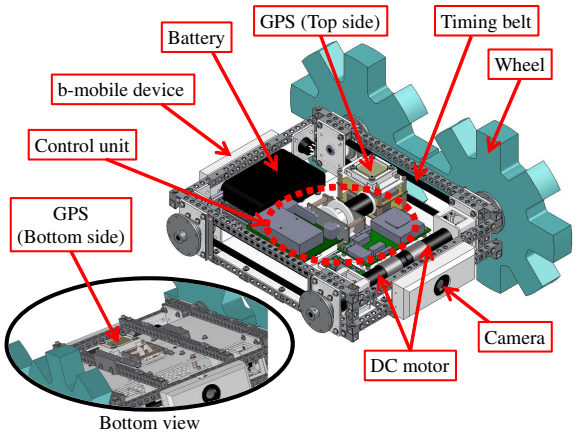

Fig. 5. 3D model of CLOVER

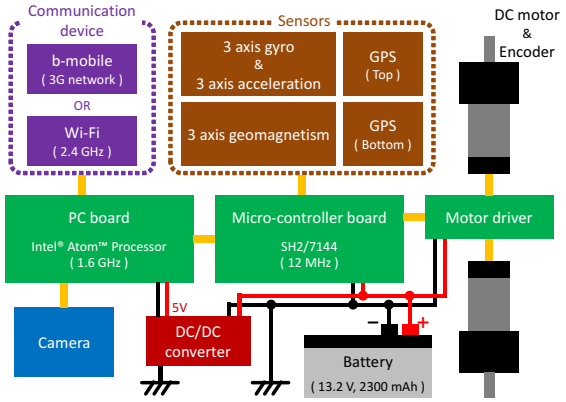

Fig. 6. CLOVER control system

B. Development of the ground robot

Target environments in this study are steep mountain slopes (over 30°), which consist of weak soil or uneven volcanic gravel. Mobile robots require effective mechanisms to traverse such challenging environments. On the other hand, the robot should be small and lightweight to be carried by UAVs. In our experience in field tests, mobile robots were in out-of-control situations on steep slopes because of rollover accidents[7]. Because of the limited camera view and time-delayed communication, we believe that it is impossible for teleoperated robots to avoid such rollover accidents. Therefore, in this research project, we developed a small, symmetrical mobile robot, as shown in Fig.4. The robot was named Compact and Lightweight teleOperation robot for Volcano ExploRation (CLOVER). Specifications of the robot are listed in Table I, and a three-dimensional (3D) model is shown in Fig.5. The robot is 450 mm in length, 360 mm in width, 220 mm in height, and approximately 3.0kg in weight. It can be carried by our multi-rotor UAV. Two wheels on each side are driven by independent DC motors (Maxon RE-max24, 11W) via a timing belt. In front of the robot, a navigation and observation camera is mounted for teleoperation using a conventional game pad. The CLOVER has a capability to climb up to 30 degrees' slope, but it depends on the target ground condition.

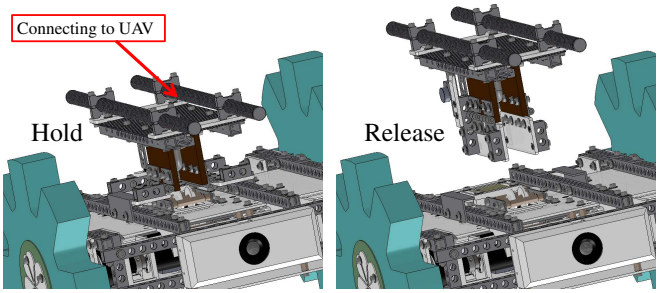

Fig. 7. Separation mechanism for UAV and CLOVER

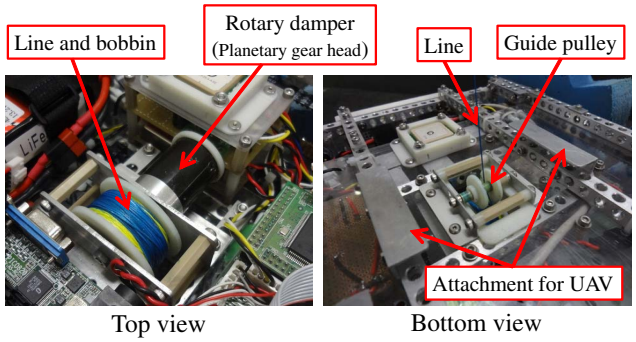

Fig. 8. Sky-crane mechanism for CLOVER

A control schematic for CLOVER is shown in Fig.6. It consists of motor drivers (3-Axes DC Power Module, produced by HiBot), a microcontroller for control of motors and sensors (SH2/7144, 12MHz, produced by RENESAS), a main control PC (PICO820 produced by Axiomtek, with an Intel®Atom™ Processor, 1.6 GHz), a four-cell lithium ferrite battery ($LiFeP0_4$, produced by A123), sensors, and a communication device. The sensors include an IMU unit (gyroscopes and accelerometers for three axes, MPU6050, produced by InvenSense), two GPS modules (LEA-6, produced by U-blox), and a camera (BSW20KM11BK, produced by Buffalo). As shown in Fig.5, the GPS modules are located on the top and bottom of the robot. Therefore, in case of rollover, the robot can continue to receive GPS signals. For the communications device, we have two choices. One is to use a b-mobile device that uses the FOMA 3G network. The other is to use a 2.4 GHz wireless LAN device (FXE1000, produced by Contec). In the case of the robot shown in Figs. 4 and 5, a b-mobile device is used for long distance communication. According to the above configuration, the robot's speed is up to 20 cm/s, but typical speed of the robot is slower than its potential.

C. Development of the sky-crane mechanism

The ground robot must be mechanically attached to the UAV during flight, and it should be released at the target GPS point. To achieve such a motion, we developed a separation mechanism. Fig.7 shows CAD models of the mechanism. The image one the left shows the configuration in the supporting phase. The attachment on the UAV is bent

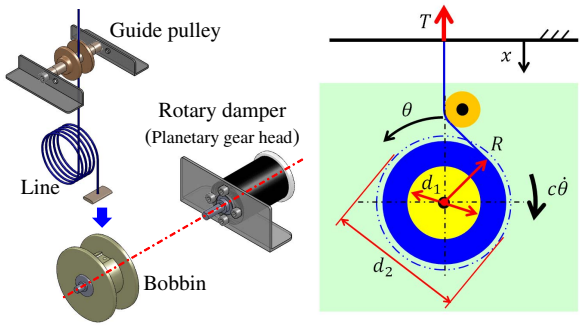

Fig. 9. Model of the drop mechanism

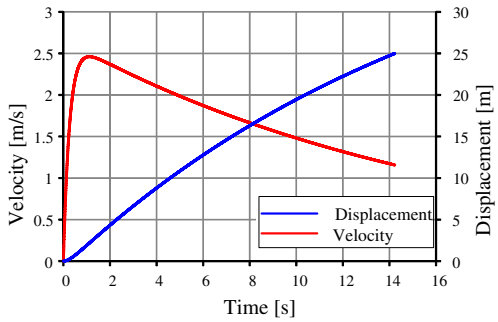

Fig. 10. Results of numerical calculations

and holds on to the hook mounted on the ground robot (shown in Fig.8-left). On the other hand, Fig.7-right shows the configuration in the released phase. The attachment of the UAV separation mechanism is straightened by a radio-controlled servomotor and released from the hook mounted on the ground robot.

To evaluate the separation mechanism, we conducted a field test in March 2013, which was reported in [8]. As the UAV hovered, CLOVER was successfully dropped from a height of 2.0 m from the ground. For this test, the UAV was manually controlled by a skilled operator with direct visual observation.

In actual operation, the UAV should be controlled autonomously because the target environment is typically too far from the operator's location for visual observation. One solution is to use a height sensor (such as a laser range sensor) to keep UAV's altitude very close to the ground, automatically. However, there is a risk of an accidental fall for the UAV caused by failed measurements because of steep slopes or rough terrain. In addition, there is a possibility of heavy surface wind. Therefore, we chose a sky-crane method, which was adopted for landing the Curiosity rover on Mars in 2012 by the NASA JPL[9]. In our case, while the multi-rotor UAV hovers 20-30 m above the ground, the ground robot is lowered slowly by a wire connected between the UAV and the ground robot.

Figure 8 shows our sky crane mechanism on CLOVER. A polyethylene fishing line (0.540 mm in diameter and 65.0 kgf maximum tensile strength) is wound on a bobbin located at the middle of the robot. The tip of the line is not fixed to the bobbin. The other tip of the line is fixed to the bottom of the multi-rotor UAV through the guide pulley. The rotation axis of the bobbin is connected to a planetary gear head as a rotary damper (damping coefficient: 4.0 Nmm/(rad/s)). After mechanical separation from the UAV, the ground robot lands passively on the surface of a steep slope at low speed. After that, the line is released from the robot by an ascending motion of the UAV (note that the tip of the line is not fixed to the bobbin on the ground robot).

D. Analysis of the sky-crane mechanism

In this subsection, the sky-crane motion is analyzed as an object is lowered. Figure 9 shows our model of the sky crane mechanism. The origin position of the coordinate system is located at the center of the hovering UAV, and the x-axis is defined as the direction perpendicular to the ground. The equation of motion for the descending object is:

$$m\ddot{x} = mg - T, \tag{1}$$

where T is defined as the tension force of the fishing line, m is the mass of the object, and g is the acceleration due to gravity. Note that the mass of the line and air resistance are ignored in this case.

The tension T is given by the following equation:

$$T = \frac{c}{R}\,\dot{\theta}, \tag{2}$$

where θ is the rotation angle of the bobbin, c is the damping coefficient of the rotary damper, and R is the ejection radius of the fishing line (the distance between the rotational axis of the bobbin and the point of application of the tension force). The mass of the bobbin and its rotational speed are negligible; therefore the moment of inertia of the bobbin is ignored in this equation.

The descent speed of the object is given by the following equation:

$$\dot{x} = R\,\dot{\theta}. \tag{3}$$

Therefore, Equations 2 and 1 can be expressed as follows:

$$T = \frac{c}{R(x)^2}\,\dot{x}, \tag{4}$$

$$\ddot{x} + \frac{1}{R(x)^2}\,\frac{c}{m}\,\dot{x} = g. \tag{5}$$

Note that R is the ejection radius of the fishing line, not the radius of the bobbin. Therefore, R is a function of x; hence $R(x)$ is used in the above equation instead of R.

Next, we consider the ejection of the fishing line. When the ejected line length is x (equal to how far the object has

TABLE II
PARAMETERS FOR NUMERICAL CALCULATIONS

m	c	d	L
3.0 kg	4.0 Nmm/(rad/s)	0.54 mm	25 m
d_1	d_2	B	k_w
25 mm	37.5 mm	15 mm	0.622

descended), the volume of the line in the bobbin V can be expressed as follows:

$$V = \frac{\pi}{4} d^2 \left(L - x\right), \tag{6}$$

where d is the diameter of the wound line and L is the length of the line. For this geometry, V can also be expressed as follows:

$$V = \frac{\pi}{4}\ k_w \left\{4R(x)^2 - {d_1}^2\right\} B, \tag{7}$$

where d_1 is the radius of the bobbin, B is the width of the bobbin, and k_w is the filling factor of the line. When $k_w = 1.0$, the line is wound tightly. In the initial condition, x is equal to zero, and $R(x)$ is expressed as the fixed parameter d_2. In this case, k_w is calculated using Equations 6 and 7, as follows:

$$k_w = \frac{d^2}{{d_2}^2 - {d_1}^2}\ \frac{L}{B} \tag{8}$$

$$R(x) = \frac{d_1}{2}\ \sqrt{1 + \frac{1}{k_w}\frac{L-x}{B}\left(\frac{d}{d_1}\right)^2}. \tag{9}$$

Using Equation 5 above, the relationship between the distance the object has been lowered, x and its velocity can be calculated.

The graph in Fig.10 shows the results of the numerical calculations using the parameters listed in Table II. According to the graph, after separation 25 m above the ground, CLOVER reaches the ground in 14 s. The descent velocity is 1.16 m/s. The descent is sufficiently slow to avoid damage to the body of the robot. Furthermore, based on Equation 4, the maximum tension force in the line is 29.8 N, which is smaller than its maximum tensile strength.

IV. Field Test at Mount Asama

To confirm the reliability of the proposed volcanic observation system, we conducted a field test from 28-30 September 2013, at Mount Asama. There were two experimental objectives: (1) operational testing of the entire observation system, which included a hexa-rotor UAV and a ground robot; and (2) long distance teleoperation of the ground robot via long distance wireless LAN communication. The flight path of the UAV and the traversal paths of the ground robot based on GPS logging data are shown in Fig.11.

V. Operation Test of the Robotic Observation System

In this test, the ZionPro800 (Fig.3) hexa-rotor UAV was used to carry a small ground robot, CLOVER, which was teleoperated via 3G communication. The departure point of the UAV was set at an elevation of 1,850 m on the route of the climb, and the release point of the ground robot was set at an elevation of 2,000 m on the steep slope (30°) of the Mount Asama. The direct distance between the departure point and the release point was approximately 600 m, and the vertical distance between them was about 200 m. The departure of the UAV was conducted manually, followed by autonomous flight to the release point (shown in Fig.12-(1)). As the UAV hovered at the release point about 20 m above the ground, the sky-crane mechanism deployed the ground robot, as shown in Fig.12-(2), (3). The ground robot landed slowly and safely after deployment of the sky-crane, as shown in Fig.12-(4). It took about 10 s for the landing. The time corresponds approximately with the theoretical data shown in Fig.10. One small concern was the effect of motion of the UAV after separation and after landing of the ground robot. In our some previous initial tests with Arduino flight microcontroller, the flight height of the UAV was changed within 50cm after separation, without any unstable mode in our visual observation. In this field test, there was no problem also. After the landing of the ground robot, we conducted teleoperation of it, as shown in Fig.12-(5). The robot was controlled from the base station that was located at the Rokuri-gahara parking lot. The base station was located at the edge of the restricted area for the case that Mount Asama erupts at a level 3 scale, 4km away from the crater of Mount Asama, and about 3km away from the robot. Fig.12-(6) shows an image obtained from the camera attached to the front of the ground robot.

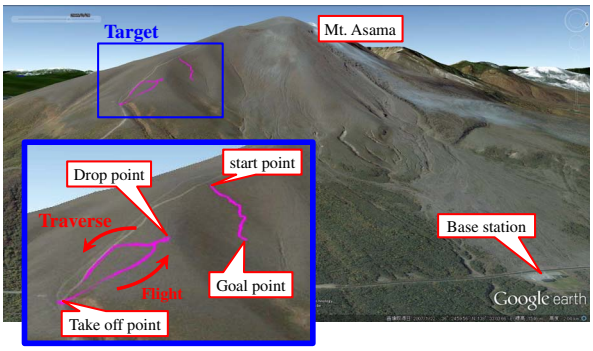

Fig. 11. Result of the Mount Asama field test

As shown in the field test described above, we confirmed the feasibility of the proposed robotic observation system in a real volcano environment. However, at this point, we have not conducted a full-scale verification test of our system for safety. In actual operation, we would have to set the departure point outside of the restricted area.

VI. Teleoperation Test of the Ground Vehicle

For the teleoperation test, CLOVER was used as the ground robot and teleoperated via a 2.4 GHz wireless LAN. In this test, we also put a teleoperation booth in the Rokuri-gahara parking lot with a 2.4 GHz wireless LAN device and a parabolic antenna. Fig.12-left shows a view from the slope of Mount Asama. We set the mission of the ground robot to visit five landmarks. One of the landmarks is shown in Fig.12-middle. The GPS coordinates of the landmarks were known, so that the operator teleoperated the ground robot using not only visual information but also GPS coordinates. Initially, the robot was located on the slope at an elevation of 2,150 m, about 3 km away from the operation booth, and reached the sixth landmark located at an elevation of 1,900 m. The total navigation length was about 400 m, and it took 30 min for navigation of all six landmarks. Fig.12-right shows a snapshot of the GUI for operators. The left

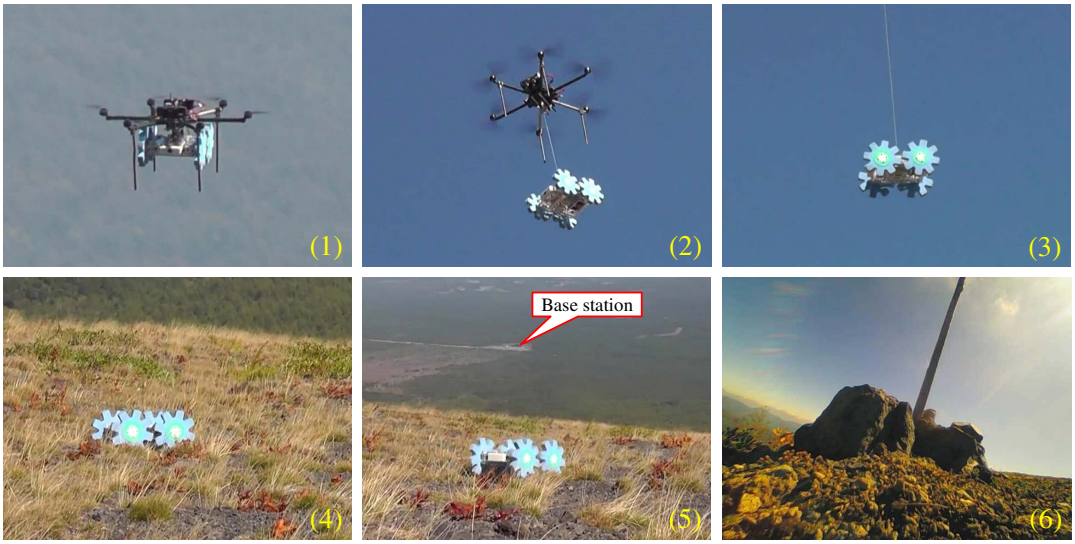

Fig. 12. Cooperative exploration of ZionPro800 and CLOVER

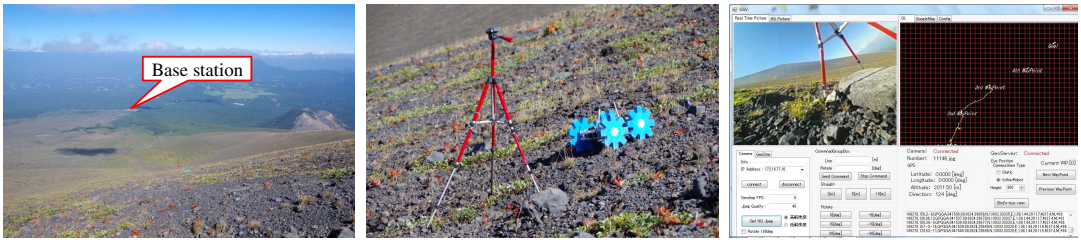

Fig. 13. Teleoperated exploration of CLOVER

of the GUI shows the camera image, and the right shows pre-registered landmarks and the robot's location. In this field test, we used camera tripods as landmarks. In actual missions, we can obtain the thicknesses of eruption products (or snow) if we install poles with a scale attachment prior to the mission, by observing the poles using a camera mounted on the robot.

Based on the two field tests described above, we believe that the proposed robotic observation system is now at an advanced stage.

VII. Conclusions

In this study, we developed a volcanic observation system that includes a multi-rotor UAV and a small, lightweight ground robot. In this system, the UAV carries the ground robot and deploys it using a sky-crane mechanism. To confirm the feasibility of the proposed system, in September 2013, we conducted field tests of the system and verified its usefulness. In future work, we will improve the observation system and conduct several field tests in actual volcanic environments to achieve practical use of the system.

ACKNOWLEDGMENT

This research project is supported by the Erosion Control Engineering Division of the R&D Institution of River Technology in the Kanto Regional Development Bureau, Ministry of Land, Infrastructure, Transport, and Tourism. To conduct the field experiment at Mount Asama, we had support from the Earthquake Research Institute of the University of Tokyo.

References

[1] J. M. Agency, "Medium- to long-term evaluation of possibility of volcanic activities in japan (japanese)," NDL Digitized Contents (info:ndljp/pid/1934666), 2009.

[2] J.E.Bares and D.S.Wettergreen, "Dante II: technical description, results, and lessons learned," *International Journal of Robotics Research*, vol. 18, no. 7, pp. 621–649, 1999.

[3] T. Arai, "Robotics and automation in Japanese construction industries," in *Proceedings of the 22nd International Symposium on Automation and Robotics in Construction*, 2005, pp. 1–5.

[4] G. Muscato, D. Caltabiano, S. Guccione, D. Longo, M. Coltelli, A. Cristaldi, E. Pecora, V. Sacco, P. Sim, G. Virk, *et al.*, "Robovolc: a robot for volcano exploration result of first test campaign," *Industrial Robot: An International Journal*, vol. 30, no. 3, pp. 231–242, 2003.

[5] G.Muscato, F.Bonaccorso, L.Cantelli, D.Longo, and C.D.Melita, "Volcanic environments: Robots for exploration and measurement," *IEEE Robotics & Automation Magazine*, vol. 19, no. 1, pp. 40–49, 2012.

[6] A. Sato, "The rmax helicopter uav," DTIC Document, Tech. Rep., 2003.

[7] K. Nagatani, H. Kinoshita, K. Yoshida, K. Tadakuma, and E. Koyanagi, "Development of leg-track hybrid locomotion to traverse loose slopes and irregular terrain," *Journal of Field Robotics*, vol. 28, no. 3, pp. 950–960, 2011.

[8] K. Nagatani, K. Akiyama, G. Yamauchi, H. Otsuka, T. Nakamura, S. Kiribayashi, K. Yoshida, Y. Hada, S. Yuta, K. Fujino, T. Izu, and R. Mackay, "Volcanic ash observation in active volcano areas using teleoperated mobile robots –introduction to our robotic-volcano-observation project and field experiments–," in *Proceedings of the 2013 IEEE Int'l Workshop on Safety, Security and Rescue Robotics*, 2013.

[9] B. D. Pollard and G. Sadowy, "Next generation millimeter-wave radar for safe planetary landing," in *Aerospace Conference, 2005 IEEE*. IEEE, 2005, pp. 1213–1219.